CROATICA CHEMICA ACTA CCACAA **74** (2) 343–357 (2001)

ISSN-0011-1643
*CCA-2736* *Original Scientific Paper*

# Enantioselectivity of *Pseudomonas cepacia* Lipase towards 2-Methyl-3(or 4)-arylalkanols: An Approach Based on the Stereoelectronic Theory and Molecular Modeling

*Sanja Tomić,* Vladimir Dobovičnik, Vitomir Šunjić, and Biserka Kojić-Prodić*

*Ruđer Bošković Institute, P. O. Box 180, HR-10002 Zagreb, Croatia*

Received December 13, 2000; revised February 14, 2001; accepted February 15, 2001

For a better understanding of the previously reported enantioselectivity of *Pseudomonas cepacia* lipase (PCL) in acylation of racemic primary alcohols, 2-methyl-3(or 4)-arylalkanols, molecular modeling of tetrahedral intermediates (TIs) at the active site was performed. The most probable conformers of TIs were elucidated and their interactions with the amino acid residues of the binding pockets at the enzyme active site were studied. The free energy difference between TIs of two enantiomers was approximated by the differences in potential energy and the solvent accesible surface area. Correlation between the Hε(His286)···Oγ(Ser87) hydrogen bond differences of diastereomeric, low energy *gauche*-TIs, and experimentally determined enantiomeric ratios was found. In agreement with the stereoelectronic theory, the *gauche*-TI precedes ester release.

*Key words*: *Pseudomonas cepacia* lipase, kinetic resolution, primary alcohols, enantioselectivity, molecular modeling, stereoelectronic theory.

## INTRODUCTION

Microbial lipases (glycerol ester hydrolases EC 3.1.1.3) are the most versatile biocatalysts and they carry out a whole range of bioconversion reactions such are hydrolysis, interesterification, esterification, alcoholysis,

* Author to whom correspondence should be addressed. (E-mail: tomic@faust.irb.hr)

acidolysis, and aminolysis. Hence, their applications in the syntheses of enantiomerically pure products for pharmaceutical and agrochemical industry are extensive. The use of lipases in detergents, leather industry, dairy industry, cosmetic and perfume industry, in environmental management, and as biosensors are examples of their wide applications.[1] In order to improve their usefulness as biocatalysts, an understanding of the lipase catalyzed reaction at molecular level is needed. In the last decade the progress was prompted by the accumulated data on three dimensional structures of lipases and their complexes, stored in the Protein Data Bank.[2]

We have selected *Pseudomonas cepacia* lipase (PCL) for our study because it shows good enantioselectivity both towards primary and secondary alcohols, contrary to most of the other microbial lipases which show low enatioselectivity towards primary alcohols. Furthermore, the active site topology of PCL obtained from X-ray structure analysis of a free enzyme and its complexes[3–6] enables reliable modeling of tetrahedral intermediates (TI) which are accepted as a good approximation of the transition state in the lipase catalyzed reactions.

This study, though a continuation of our experimental and computational studies of lipase catalyzed acylations of specific classes of conformational flexible substrates,[7,8] was specifically prompted by the set of interesting results concerning enantioselectivity in acylation of a set of primary alcohols, reported by Ferraboschi *et al*.[9,10] a few years ago. Besides, binding of primary alcohols into the active site of PCL has been less studied[11,12] than that of secondary alcohols.[12–27] The existing empirical rules that predict the faster reacting enantiomer in the lipase catalyzed esterification of chiral alcohols[11,28,29] are more reliable for secondary than for primary alcohols.[11] Finally, molecular modeling of the tetrahedral intermediates of a series of primary and secondary alcohol esters revealed different modes of binding of substrates into large and small pockets of the PCL binding site.[11–27]

## METHODS

### *Hardware and Software*

All calculations were performed on a Silicon Graphics workstation Octane/R10K under the IRIX (version 6.5) operating system. The programs Insight II, version 98.0,[30] and Discover, version 2.9.7,[31] were used.

### *Modeling of the Complexes*

Two starting structures were used: the crystal structure of the PCL-inhibitor complex, accession code: 5LIP[3] in the first stage of molecular modeling; and later the crystal structure of the complex of PCL with the *sec*-alcohol-like inhibitor.[6]

The acyl-enzyme structure was built using the topology of the inhibitor bound to PCL, *i.e.* phosphorus was replaced by carbonyl carbon covalently bound to Ser87. Hydrogens were added using the Biopolymer module in the program INSIGHT II,[30] utilizing the pH value at which the complex was formed and crystallized: 4.0 (5LIP) and 7.5 (PCL–*sec*-alcohol as inhibitor). The protonation of histidines (either Nδ1 or Nε2) was adjusted manually, depending on the possibilities of hydrogen bond formation; the protonated form of the catalytic His286 was used. Water molecules were removed from the crystal structures. Parameterization was performed in the AMBER[32] force field. In order to remove internal strains, the initial structures were energy minimized without constraints by the conjugated gradients algorithm. A distance dependent dielectric constant ($\varepsilon = 4r$) and scaling (0.5) of the 1–4 interaction was used.

## *Conformational Search*

Optimized structures of both enantiomers of substrates **1**–**6** (Scheme 1) were bound to acylated Ser87.

Charges of the TI core were determined using MOPAC MNDO-ESP calculations[33] and adjusted to the force field parameters: –0.57, 0.75, –0.77 and –0.57 for alcohol O(alcohol), $C_T$, oxyanion O* and O(Ser87), respectively.

Systematic conformational search protocols were employed to determine the low energy minima of these complexes. Dihedrals T1, T2 and Tkc (Figure 1) were varied from 0° to 360° in 30° steps. Each rotation was followed by a limited minimization procedure (combined steepest descent and conjugate gradients). Conformations obtained by the conformational search were scanned and those reaching the given structural and energetic criteria were energy minimized until convergence of 0.4 kJ $mol^{-1}$ $Å^{-1}$. The first selection was performed on the basis of a rather arbitrary energy threshold of 400 kJ $mol^{-1}$. In the second step, the complexes containing H-bonds characteristic of TI were selected (see Results). Stability of the conformers was further checked by the molecular dynamics (MD) simulations at room temperature. The backbone was constrained during the conformational search, final energy minimization and MD simulations. For some complexes (PCL-2), additional conformational search was performed by MD simulations at increasing temperatures (300–500 K). Using MD simulation at high temperature we tried to figure out the possibility of transitions between the minima found by systematic conformational search and to find additional, energetically close minima of the complex. In this way, the most probable conformations of the bound substrates were determined.

During conformational search and optimization, the lipase backbone was kept fixed, since the structures of free PCL and its complex with inhibitor revealed insignificant difference in the backbone conformation.[6]

## *Solvent Accessible Surface Evaluation*

Solvent accessible surface area (SASA) of the lowest energy *anti*- and *gauche*-TIs was calculated using the Naccess program.[34] Difference of the SASA per residue between diastereomeric TIs was determined using an in-house program. Only the diastereomers with the same orientation of the Oγ(Ser87)-$C_T$-O(alcohol)-R dihedral angle were considered. The largest difference in the non-polar SASA was determined for the methyl group bound to the stereogenic center in **1**–**6**.

## RESULTS AND DISCUSSION

Molecular modeling was used to explain the surprisingly high difference in enantioselectivity in acetylation of a series of 2-methyl-3(or 4)-arylalkanols **1**–**6** by PCL, (Scheme 1) found experimentally by Ferraboschi *et al.*[9,10] These authors observed that acetylation of substrates **1**–**3**, having an aryl group on the carbon vicinal to the stereogenic center, proceeded with low enantioselectivity (*E*-values 2–9), whereas substrates **4**–**6**, with an aryl group

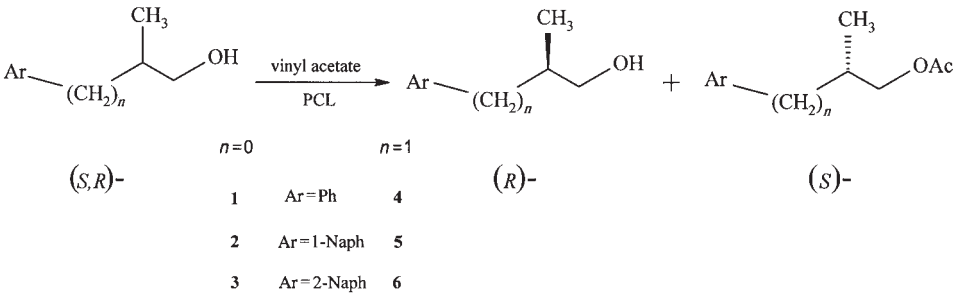


Scheme 1

separated from the stereogenic center by an additional methylene group, were acetylated with much higher enantioselectivity (*E*-values 45–170), Table I. In all cases, (*S*)-enantiomer was preferentially acetylated.

The authors suggest that these results might be explained in terms of interactions between the aromatic moiety of substrates and aromatic amino acids at the PCL binding site. We approached these interesting results with a combined study of the diastereomeric enzyme-TIs complexes potential energy surfaces, their solvent accessible surface area (SASA), and specific interactions with the α-amino acid residues in the PCL active site.

The influence of the starting structure and minimization procedure on the results of molecular modeling was investigated before starting the demanding conformational search.

Starting from the two crystal structures of PCL-substrate complexes, PDB code 5LIP[3] and the one recently determined in our laboratory,[6] TIs of both enantiomers of substrates **2** and **3** were modeled. Two different starting structures revealed the same binding modes with different absolute energies, as shown in Table II. The same set of conformers was determined in both cases and the relative energies calculated for equivalent conformers were similar.

TABLE I

Enantioselectivity parameters for acetylation of primary alcohols, catalyzed by PCL[9,10]

| Compound | Time / h | Yield[a] / % | ee[b] / % | *E* | Configuration |
|---|---|---|---|---|---|
| **1** | 3 | 40 | 20 | 1.8 | *S* |
| | 8 | 60 | 20 | | *R* |
| **2** | 86 | 35 | 72 | 9 | *S* |
| | 97 | 57 | 70 | | *R* |
| **3** | 16 | 32 | 62 | 6 | *S* |
| | 22 | 69 | 65 | | *R* |
| **4** | 1 | 40 | >98 | 172 | *S* |
| | 2 | 60 | >98 | | *R* |
| **5** | 4 | 30 | >98 | 150 | *S* |
| | 23 | 66 | >98 | | *R* |
| **6** | 3 | 40 | 92 | 45 | *S* |
| | 7 | 60 | 85 | | *R* |

[a] Percentage of primary alcohol converted to acetate in the given time.
[b] Upper numbers refer to acetate (*S*), and lower to unreacted alcohol (*R*).

TABLE II

Energy and conformations of the enzyme-TI complexes obtained using two different starting structures (5LIP[3] and PCL complex with *sec*-alcohol-like inhibitor)[6]

| Complex name | Absolute energy / kJ mol$^{-1}$ | T1 | Tkc |
|---|---|---|---|
| ZAG-(*R*)-**2**-g | –18371 | 177 | 168 |
| ZAG-(*S*)-**2**-g | –18383 | –175 | 165 |
| 5LIP-(*R*)-**2**-g | –14818 | 176 | 173 |
| 5LIP-(*S*)-**2**-g | –14841 | –177 | 168 |
| ZAG-(*R*)-**3**-g | –18510 | –177 | 178 |
| ZAG-(*S*)-**3**-g | –18511 | –176 | 179 |
| 5LIP-(*R*)-**3**-g | –14867 | 177 | 178 |
| 5LIP-(*S*)-**3**-g | –14868 | –178 | 170 |

Although the choice of the starting structure and optimization method is not critical for the final results, only the energies obtained by the same procedure can be compared.

The geometry of the TI core is defined by the position of the oxygen ion in the oxyanion hole and by orientation of the alkyl group (in our case $CH_3$) in the hydrophobic HA pocket, close to Pro113, Val266 and Val267. Such arrangement revealed the *R* configuration of the tetrahedral carbon bound to the Ser87 oxygen for all the primary alcohols studied (Scheme 1).

Using systematic conformational search, molecular mechanics, and molecular dynamic simulations, a number of low energy binding modes were found for each pair of enantiomers of **1**–**6**. However, only those binding modes in which hydrogen bonds required for the catalytic reaction are present are considered TIs; Oδ2(Asp264)···Hδ1(His286), Hε(His286)···Oγ(Ser87), Hε(His286)···O(alcohol) and hydrogen bonds between oxyanion (O*) and protonated amide nitrogen of L17 and Q88. The lowest energy TIs are given in Tables III and IV.

TABLE III

Structures and relative energies of the enzyme tetrahedral intermediate complexes of primary alcohols **1**-**6** with *gauche* conformation of dihedral O(Ser87)-$C_T$-O(alcohol)-R[a]

| Complex name | Relative energy kJ mol$^{-1}$ | T1 | T2 | Tkc | Hydrogen bonds[b] Å | |
|---|---|---|---|---|---|---|
| (*R*)-**1**-g1 | 3 | –168 | | –176 | 2.16 | 2.00 |
| (*R*)-**1**-g2 | 13 | 50 | | 164 | 2.34 | 1.97 |
| (*S*)-**1**-g1 | 0 | –174 | | 170 | 2.41 | 1.93 |
| (*R*)-**2**-g1 | 17 | –83 | | –169 | 2.40 | 1.95 |
| (*R*)-**2**-g2 | 65 | 177 | | 168 | 2.21 | 2.05 |
| (*S*)-**2**-g1 | 55 | –53 | | 177 | 2.13 | 1.97 |
| (*S*)-**2**-g2 | 53 | –175 | | 165 | 2.43 | 2.07 |
| (*R*)-**3**-g1 | 1 | –177 | | 178 | 2.18 | 2.04 |
| (*S*)-**3**-g1 | 0 | –176 | | 179 | 2.45 | 1.97 |
| (*R*)-**4**-g1 | 10 | –172 | –161 | 178 | 2.09 | 2.16 |
| (*S*)-**4**-g1 | 11 | 92 | –57 | 178 | 2.10 | 2.08 |
| (*S*)-**4**-g2 | 6 | –177 | –177 | 167 | 2.27 | 2.05 |
| (*R*)-**5**-g1 | 9 | –162 | –152 | –179 | 2.08 | 2.23 |
| (*S*)-**5**-g1 | 9 | –177 | –177 | 167 | 2.26 | 2.07 |
| (*S*)-**5**-g2 | 12 | –160 | –166 | 169 | 2.24 | 2.05 |
| (*R*)-**6**-g1 | 15 | –174 | 163 | 176 | 2.10 | 2.15 |
| (*S*)-**6**-g1 | 14 | –177 | –177 | –167 | 2.26 | 2.07 |

[a] For definition of dihedral angles see Figure 1.
[b] The first column is His286-O(alcohol) and the second His286-Ser87 hydrogen bond distance.

TABLE IV

Structures and relative energies of the enzyme tetrahedral intermediate complexes of primary alcohols **1-6** with *anti* conformation of dihedral O(Ser87)-$C_T$-O(alcohol)-R[a]

| Complex name | Relative energy kJ mol$^{-1}$ | T1 | T2 | Tkc | Hydrogen bonds[b] Å | |
|---|---|---|---|---|---|---|
| (*R*)-**1**-a1 | 8 | –178 | | 176 | 2.46 | 1.97 |
| (*S*)-**1**-a1 | 16 | –174 | | 179 | 2.10 | 2.04 |
| (*R*)-**2**-a1 | 0 | 179 | | –174 | 2.40 | 2.01 |
| (*S*)-**2**-a1 | 21 | –173 | | –165 | 2.07 | 2.05 |
| (*R*)-**3**-a1 | 25 | 179 | | –178 | 2.43 | 1.98 |
| (*S*)-**3**-a1 | 23 | –167 | | –178 | 2.19 | 2.00 |
| (*R*)-**4**-a1 | 0 | –173 | 148 | 175 | 2.02 | 2.56 |
| (*S*)-**4**-a1 | 6 | 176 | –171 | 177 | 2.06 | 2.15 |
| (*R*)-**5**-a1 | 3 | –173 | 136 | 175 | 2.06 | 2.11 |
| (*R*)-**5**-a2 | 0 | –173 | –179 | –175 | 2.25 | 2.07 |
| (*S*)-**5**-a1 | 9 | 176 | 142 | 179 | 2.12 | 2.13 |
| (*S*)-**5**-a2 | 1 | 180 | –172 | –169 | 2.05 | 2.14 |
| (*R*)-**6**-a1 | 26 | –170 | –75 | –163 | 2.08 | 2.15 |
| (*R*)-**6**-a2 | 6 | –176 | 131 | 179 | 2.06 | 2.12 |
| (*R*)-**6**-a3 | 6 | 176 | 166 | –178 | 2.26 | 2.07 |
| (*S*)-**6**-a1 | 14 | 72 | –173 | –179 | 2.06 | 2.15 |
| (*S*)-**6**-a2 | 6 | 178 | 143 | –180 | 2.22 | 2.08 |
| (*S*)-**6**-a3 | 0 | 172 | 71 | –180 | 2.22 | 2.08 |
| (*S*)-**6**-a4 | 14 | 160 | –177 | 174 | 2.06 | 2.13 |

[a] For definition of dihedral angles see Figure 1.
[b] The first column is His286-O(alcohol) and the second His286-Ser87 hydrogen bond distance.

Apparently, the low energy conformers of both enantiomers have a similar orientation of the large substituent (L = $Ar(CH_2)_n$), *i.e.* two enantiomers have the so-called L-alignment,[12] see Figure 1. According to these results, the entropy difference between diastereomeric enzyme-TI complexes can be neglected in evaluation of the free energy difference.

The same type of alignment of two enantiomers of primary alcohols in the PCL active site was found by Tuomi and Kazlauskas.[11] We have ob-

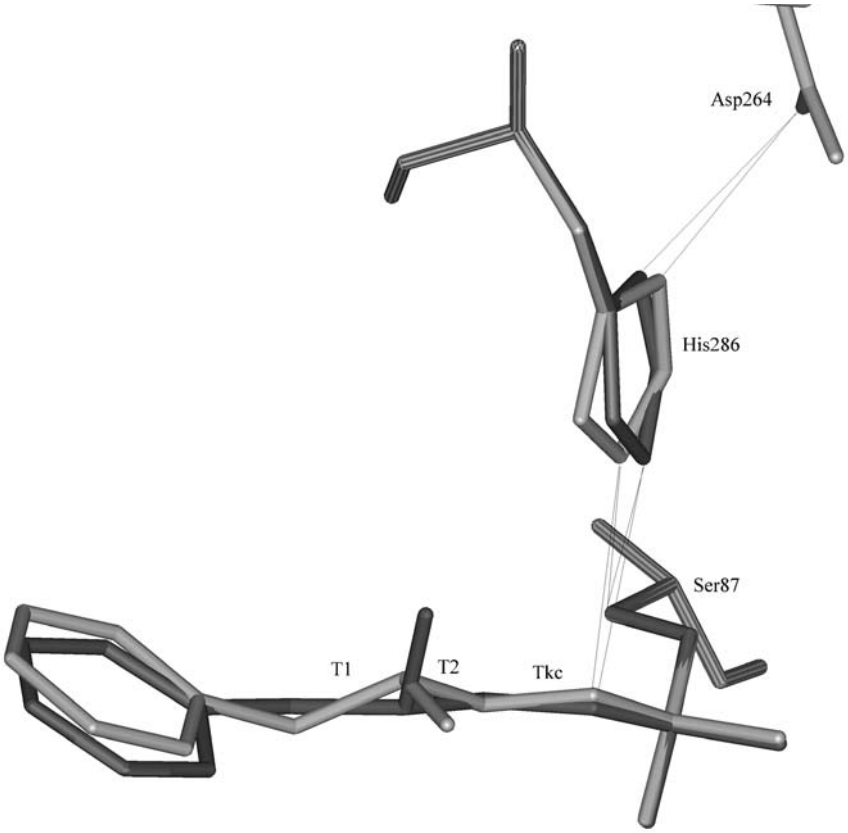


Figure 1. Superposition of the lowest energy enzyme tetrahedral intermediates of (*S*)-**4** (black) and (*R*)-**4** (gray) complexes with the *gauche* conformation of the dihedral O(Ser87)-$C_T$-O(alcohol)-R. The hydrogen bond network necessary for the catalytic reaction is displayed and torsion angles changed during systematic conformational search are designated: T1 = Ar-C-C-C($O^a$), T2 = C-C-C-O, Tkc = C-$CH_2$-O-C(chiral). [a]TIs with substrates **1**-**3**. These substrates do not have T2.

served that the large substituent of each enantiomer of **1**–**6** can adopt a few different orientations in the active site. With regard to these orientations, three main groups of low energy binding modes were observed: a) with $Ar(CH_2)_n$ accommodated within stereoselective, HH, pocket, b) with $Ar(CH_2)_n$ pointing out of the active site, and c) with $Ar(CH_2)_n$ only partly occupying the stereoselective pocket, Figure 2.

The TIs of **1**–**6** with the large group accommodated in the stereoselective HH pocket, which is partly hydrophilic, have the lowest potential energy due to a number of stabilizing van der Waals interactions. Most of these inter-

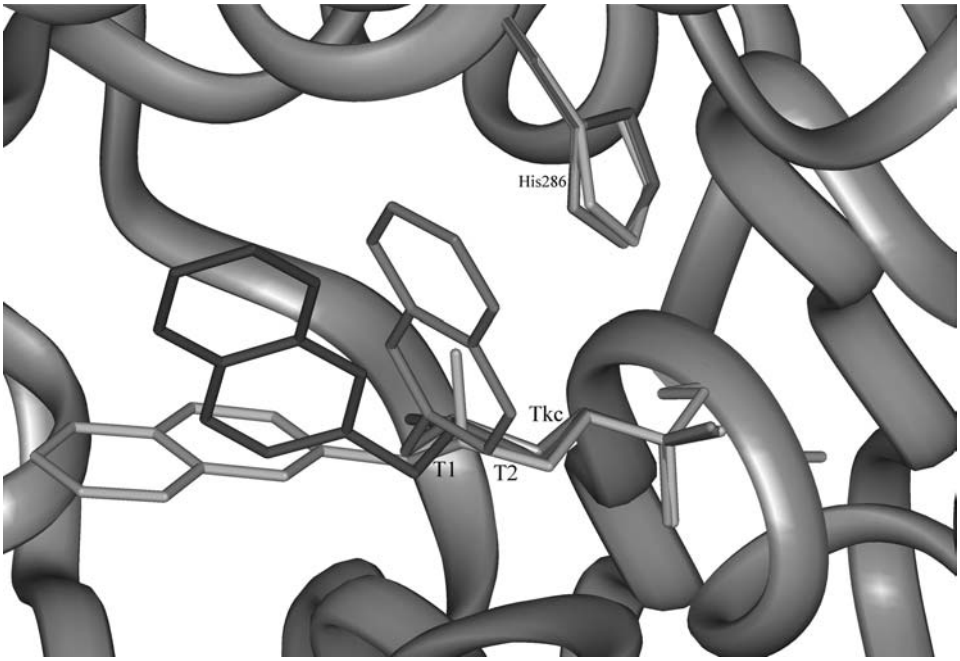


Figure 2. Superposition of three different, low energy binding modes determined for (*S*)-**6**. The protein backbone is given in ribbon representation.

actions are hydrophobic in nature, like the interactions between substrates and the side chains of Leu27, Leu287, Ile290, Leu293. The π–π interactions, discussed by Ferraboschi *et al.*,[9,10] are significant in this particular binding mode. The aromatic ring planes of the substrates are approximately planar with the phenyl groups of both Tyr23 and Tyr29 (angle between the planes ranging from 0° to 30°) and the shortest distance between the geometrical mean of one aromatic ring and hydrogen atoms of the other is about 3Å, *i.e.* geometrical means (GM) of the aromatic systems are shifted about 1.9–2.5 Å to each other. Similar geometrical arrangements between aromatic rings are found in some crystal structures.[35] In such an arrangement with aromatic systems overlapping only at their edges, the CH/π interaction is the most significant.[36] However, the geometrical arrangement of aromatic systems and the strength of the interactions are similar for both enantiomers; it seems therefore that interactions between aromatic amino acid residues and the substrate aryl ring are not responsible for the much higher enantioselectivity in acetylation of substrates **4**–**6**. This result is not unexpected in view of the contradictory findings[11,37] concerning the influence of π–π interactions on enantioselectivity. Whereas Botta *et al.*[37] pointed to the importance of these

interactions in the stabilization of the lipase-arylpropionic ester complexes, Tuomi and Kazlauskas[11] revealed the drawback of these interactions for the acylation rate.

The structural factor that seems to be correlated with the measured enantioselectivity *E*, is the difference in the His286···Ser87 hydrogen bond distances, determined for the lowest energy diastereomeric TIs, with *gauche* conformation of the dihedral O(Ser87)-$C_T$-O(alcohol)-R, Figure 3.

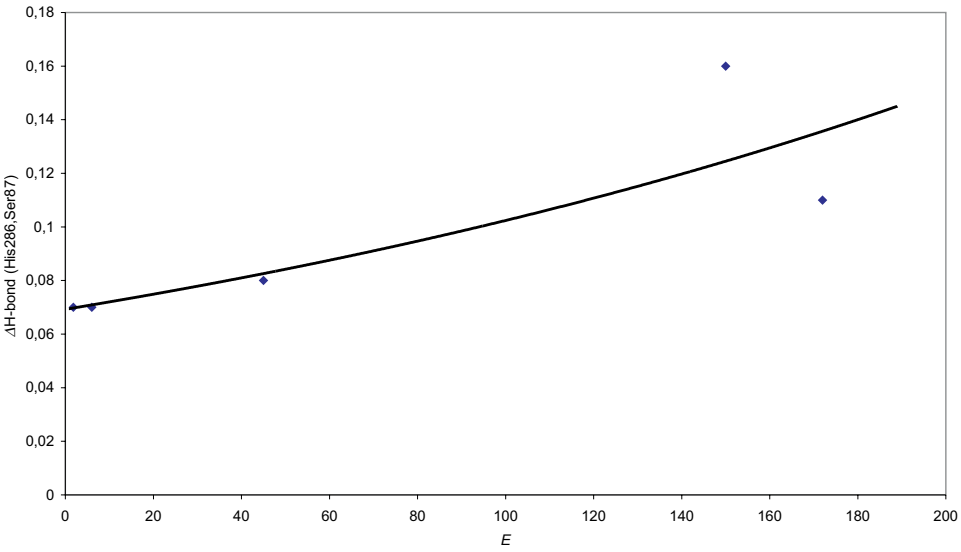


Figure 3. Measured enantiomeric ratios *E vs*. differences of the His286···Ser87 hydrogen bond distance in the (*R*)- and (*S*)-enzyme-*gauche*-TI complexes of **1**, **3**-**6**.

Regarding the conformation of this dihedral angle, two possible conformations of the tetrahedral intermediate were identified: +*gauche* and *anti,* see Tables III and IV, respectively, and Figure 4.

The –*gauche* conformation of the faster enantiomer is not allowed because of the architecture of the active site, *i.e*. due to strong steric hindrance of this enantiomer with the wall of the binding pocket. We also tried to model TI with the O(Ser87)-$C_T$-O(alcohol)-R dihedral angle about 120°, as it is found in the crystal structure,[6] but it turned out that this conformation is unstable; during optimization it changes either to +*gauche* or *anti*.

It is generally accepted that, in the process of transesterification, the leaving transition state, in which the hydrogen bond Hε(His286)···Oγ(Ser87)

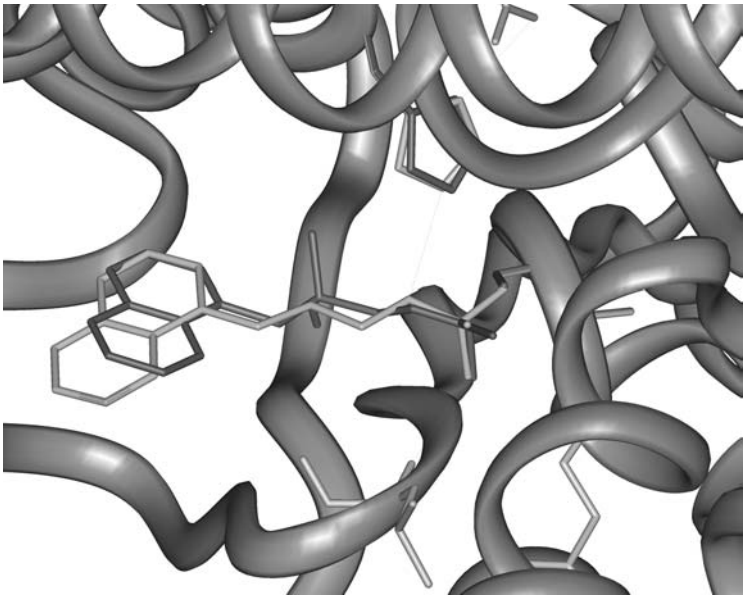

Figure 4. Superposition of the lowest energy enzyme tetrahedral intermediates of (*S*)-**5** complexes with the *gauche* (black) and *anti* (gray) conformation of the dihedral angle O(Ser87)-$C_T$-O(alcohol)-R. The protein backbone is given in ribbon representation.

is very strong and Hε(His286)···O(alcohol) is broken, is rate determining.[29] The stereoelectronic theory[38] predicts that the C-O bond can be efficiently cleaved only if both remaining geminal oxygens have lone pairs *antiperiplanar* to the breaking bond. In the catalyzed ester hydrolysis this condition is satisfied for both *gauche* and *anti* conformations of the TI, Figure 4, but in the transesterification process this condition is satisfied only for the *gauche*-TI. According to this theory, the transesterification reaction can proceed only if the conformation of the dihedral O(Ser87)-$C_T$-O(alcohol)-R is *gauche*.

From Tables III and IV one can see that the H-bond between the catalytic His286 and Ser87 is shorter in *gauche*-TIs for the preferred (*S*)-enantiomers; apparently these TIs could be considered as the approximation of the leaving transition state. In view of these findings, we tried to estimate the free energy difference of diastereomeric *gauche*-TIs. The potential energy difference between diastereomeric *gauche*-TIs of primary alcohols is small, Table III, and in most cases correctly predicts the preferred enantiomer; quantitative estimation of the enantioselectivity is not possible, however.

To better estimate the free energy difference, an approximate difference in the desolvation free energies of two enantiomers was calculated. By inspection of the differences in solvent accessible surface areas (SASA) of TIs, we noticed that the methyl group in the alcohol stereogenic center is much better desolvated in the (*S*)- than in the (*R*)-enantiomers, regardless of *gauche*- or *anti*-configuration (see Table V). For compounds **4** and **5**, the solvent accessible surface area differences are the largest, in accord with the very high enantiomeric ratio *E*.[9,10] According to recent measurements,[39,40] the energy of the transfer of a methyl group from the organic phase to water is about 4 kJ mol$^{-1}$ and the solvent accessible surface area (SASA) of such a

TABLE V

Differences between the methyl-group solvent accessible surface area of the lowest energy conformers of the (*R*)- and (*S*)-enantiomer TIs in the PCL active site

| Compound | ΔSASA / Å$^2$ | |
|---|---|---|
| | *g*-TI | *a*-TI |
| **1** | 2 | 8 |
| **2** | 3 | 0 |
| **3** | 1 | 1 |
| **4** | 18 | 7 |
| **5** | 5 | 13 |
| **6** | 0 | 6 |

methyl group is about 25 Å$^2$. Disregarding the differences in polarizability of the lipase and the organic system used in the experimental measurements, we can approximate the difference between the solvation free energy of two diastereomers by the product of the surface ratio (difference/total) and empirically determined solvation energy. Based on this assumption the free energy of *gauche*-TI of (*S*)-**4** ((*S*)-**4**-g2) decreases relative to *gauche*-TI of (*R*)-**4** ((*R*)-**4**-g1) by about 3 kJ mol$^{-1}$, and the free energy of *anti*-TI of (*S*)-**5** ((*S*)-**5**-a2) decreases relative to *anti*-TI of (*R*)-**5** ((*R*)-**5**-a2) by about 2 kJ mol$^{-1}$. In the *gauche* conformation of TIs of the (*S*)-enantiomer of **1**, **3**–**6**, the methyl group pushes the imidazole ring of His286 towards catalytic Ser87, Figure 4. This leads to a decrease of the distance between the serine carbonyl oxygen and imidazole hydrogen and an increase of the strength of the Hε(His286)···Oγ(Ser87) hydrogen bond, whereas the strength of the Hε(His286)···O(alcohol) hydrogen bond decreases.

We also observed that conversion times have a broad range (see Table I) and can be qualitatively correlated with the energy difference between *gauche-* and *anti-*TIs of the (*S*)-enantiomer. We assume that the acetylation rate could be significantly decreased if a number of low energy *anti* tetrahedral intermediates exist. Namely, from these intermediates the reaction cannot easily proceed because of the unfavorable position of the lone pairs on geminal oxygens. While both *gauche-* and *anti-*TIs were similar in energy for most compounds, the energy of the *anti-*TIs of **2** was found for both enantiomers to be significantly lower than for *gauche-*TIs and, as expected, the conversion time of this compound was extremely long.

## CONCLUSION

The lowest energy TI of **1–6** are those with $Ar(CH_2)_n$ accommodated in the HH pocket. Interactions between the aromatic unit of this larger group and aromatic amino acid residues of the PCL active site are significant in these complexes. Though weaker for **4–6** than for the other substrates, they cannot explain the enhancement of experimentally determined enantioselectivity measured for these compounds.

Acetylation of **1–6** catalyzed by PLC probably proceeds *via* the *gauche* conformation of TI, which collapses to the acylated products faster than other TIs. Methyl group in the stereogenic center of the more reactive (*S*)-enantiomers is better desolvated, and in the enzyme-*gauche*-TI complexes it pushes the imidazole ring of the catalytic His286 towards Ser87. As a result, the Hε2···Oγ hydrogen bond between these two residues becomes stronger and facilitates the proton transfer from H286 to Ser87, cleavage of the C-O bond, and ester release. The difference between the hydrogen bond His286···Ser87 distance in (*R*)- and (*S*)-enzyme-*gauche*-TI complexes is well correlated with the measured enantiomeric ratio *E*.

*Acknowledgements.* – S. Tomić thanks the Alexander von Humbold Foundation for the donated OCTANE-SGI workstation. This work was supported by grants 00980608 from the Ministry of Science and Technology of Croatia and Volkswagen-Stiftung, I/72566, Germany.

## REFERENCES

1. A. Pandey, S. Benjamin, C. R. Soccol, P. Nigam, N. Krieger, and V. T. Soccol, *Biotechnol. Appl. Biochem*. **29** (1999) 119–131.
2. H. M. Berman, J. Westbrook, Z. Feng, G. Gilliland, T. N. Bhat, H. Weissig, and I. N. Shindyalova, *Nucleic Acids Res.* **28** (2000) 235–242.

3. J. D. Schrag, Y. Li, M. Cygler, D. Lang, T. Burgdorf, H.-J. Hecht, R. Schmid, D. Schomburg, T. J. Rydel, J. D. Oliver, L. C. Strickland, C. M. Dunaway, S. B. Larson, J. Day, and A. McPherson, *Structure* **5** (1997) 187–202.
4. K. K. Kim, H. K. Song, D. H. Shin, K. Y. Hwang, and S. W. Suh, *Structure* **5** (1997) 173–185.
5. D. A. Lang, M. L. M. Mannesse, G. H. de Haas, H. M. Verheij, and B. W. Dijkstra, *Eur. J. Biochem*. **254** (1998) 333–340.
6. M. Luić, S. Tomić, I. Leščić, E. Ljubović, D. Šepac,V. Šunjić, Lj. Vitale, W. Saenger, and B. Kojić-Prodić, *Eur. J. Biochem.* submitted.
7. E. Ljubović and V. Šunjić, *Tetrahedron: Asymm*. **8** (1997)1–4.
8. E. Ljubović and V. Šunjić, *Croat. Chem. Acta* **71** (1998) 99–117.
9. P. Ferraboschi, S. Casati, A. Manzocchi, and E. Santaniello, *Tetrahedron: Asymm.* **6** (1995) 1521–1524.
10. P. Ferraboschi, S. Casati, S. De Grandi, P. Grisenti, and E. Santaniello, *Biocatalysis* **10** (1994) 279–288.
11. W. V. Tuomi and R. J. Kazlauskas, *J. Org. Chem*. **64** (1999) 2638–2647.
12. J. Zuegg, H. Hönig, J. D. Schrag, and M. Cygler, *J. Mol. Catalysis B: Enzymatic* **3** (1997) 83–98.
13. R. J. Kazlauskas, *Trends Biotechnol*. **12** (1994) 464–472.
14. P. Grochulski, F. Bouthillier, R. J. Kazlauskas, A. N. Serreqi, J. D. Schrag, E. Ziomek, and M. Cygler, *Biochemsitry* **33** (1994) 3494–3500.
15. T. Norin, F. Haeffner, K. Hult, and O. Edholm, *Biophysical J*. **67** (1994) 548–559.
16. M. Holmquist, F. Haeffner, T. Norin, and K. Hult, *Protein Sci.* **5** (1996) 83–88.
17. A. T. Yagnik, J. A. Littlechild, and N. J. Turner, *J. Compt.-Aided Mol. Design* **11** (1997) 256–264.
18. G. H. Peters, D. M. F. van Aalten, A. Svendsen, and R. Bywater, *Protein Eng.* **10** (1997) 149–158.
19. T. Ema, M. Jittani, T. Sakai, and M. Utaka, *Tetrahedron Lett.* **39** (1998) 6311–6314.
20. C. Orrenius, F. Haeffner, D. Rotticci, N. Öhrner, T. Norin, and K. Hult, *Biocatal. Biotransform.* **16** (1998) 1–15.
21. F. Haeffner, T. Norin, and K. Hult, *Biophys. J*. **74** (1998) 1251–1262.
22. H. Scheib, J. Pleiss, P. Stadler, A. Kovač, A. P. Potthoff, L. Haalck, F. Spener, F. Paltauf, and R. D. Schmid, *Protein Eng.* **11** (1998) 675–682.
23. X. Grabuleda, C. Jaime, and A. Guerrero, *Tetrahedron: Asymm*. **8** (1997) 3675–3683.
24. A. N. E. Weissfloch and R. J. Kazlauskas, *J. Org. Chem*. **60** (1995) 6959–6969.
25. A. Tafi, A. van Almsick, F. Corelli, M. Crusco, K. E. Laumen, M. P. Schneider, and M. Botta, *J. Org. Chem*. **65** (2000) 3659–3665.
26. M. Shokhen and A. Albeck, *Proteins: Struct. Func. Genet.* **40** (2000) 154–167.
27. T. Schulz, J. Pleiss, and R. D. Schmid, *Protein Sci.* **9** (2000) 1053–1062.
28. M. Cygler, P. Grochulski, R. J. Kazlauskas, J. D. Schrag, F. Bouthillier, B. Rubin, A. N. Serreqi, and A. K. Gupta, *J. Am. Chem. Soc*. **116** (1994) 3180–3186.
29. U. T. Bornscheuer and R. J. Kazlauskas, *Hydrolases in Organic Synthesis*, Wiley-VCH, Weinheim, 1999.
30. INSIGHT970, Release 97.0 edit. MSI, San Diego, 1997.
31. DISCOVER 2.9.7, Release edit. MSI, San Diego, 1997.

32. W. D. Cornell, P. Cieplak, C. I. Payly, I. R. Gould, K. M. Merz, D. M. Ferguson, D. C. Spellmeyer, T. Fox, J. W. Caldwell, and P. A. Kollman, *J. Am. Chem. Soc.* **117** (1995) 5179–5197.
33. MOPAC 6.0, QCPE Program, Indiana University, 1990.
34. S. J. Hubbard and J. M. Thornton, NACCESS, Department of Biochemistry and Molecular Biology, University College London, London, 1993.
35. R. Kiralj, PhD Thesis, University of Zagreb, Zagreb, 1999.
36. M. Nishiom M. Hirota, and Y. Umezawa, *The CH/π Interaction: Evidence, Nature and Consequences*, in: A. P. Marchand (Ed.), *Series Methods in Stereochemical Analysis*, Wiley-VCH, New York, 1998.
37. M. Botta, E. Cernia, F. Corelli, F. Manetti, and S. Soro, *Biochim. Biophys. Acta* **1337** (1997) 302–310.
38. T. Ema, J. Kobayashi, S. Maena, T. Sakai, and M. Utaka, *Bull. Chem. Soc. Jpn.* **71** (1998) 443–453.
39. W. C. Wimley, T. P. Creamer, and S. H. White, *Biochemistry* **35** (1996) 5109–5124.
40. P. Shih, L. G. Pedersen, P. R. Gibbs, and R. Wolfenden, *J. Mol. Biol.* **280** (1998) 421–430.

## SAŽETAK

### Enantioselektivnost lipaze *Pseudomonas cepacia* prema 2-metil-3(ili 4)-arilalkanolima: pristup temeljen na stereoelektronskoj teoriji i molekulskom modeliranju

*Sanja Tomić, Vladimir Dobovičnik, Vitomir Šunjić i Biserka Kojić-Prodić*

Za bolje razumijevanje ranije priopćene enantioselektivnosti lipaze *Pseudomonas cepacia* (PCL) u aciliranju racemičnih primarnih alkohola, 2-metil-3(ili 4)-arilalkanola, provedeno je molekulsko modeliranje tetraedalnih intermedijara (TI) u aktivnom mjestu. Određeni su najvjerojatniji konformeri za TI i proučavane su njihove interakcije s aminokiselinskim ostatcima unutar veznih džepova aktivnog mjesta enzima. Razlika Gibbsovih energija tetraedalnih intermedijara dvaju enantiomera približno je dana kao zbroj razlika njihovih potencijalnih energija i slobodnih energija otapanja. Nađena je ovisnost razlike duljina vodikove veze Hε(His286)···Oγ(Ser87) za dijastereomerna, niskoenergijska *gauche* prijelazna stanja (*gauche*-TI) i eksperimentalno utvrđenog enantiomernog omjera. U skladu sa stereoelektronskom teorijom, *gauche*-TI prethodi oslobađanju estera.